Axis-switching of a micro-jet

Juan Martin Cabaleiro and Jean-Luc Aider

Citation: Physics of Fluids (1994-present) **26**, 031702 (2014); doi: 10.1063/1.4868256
View online: http://dx.doi.org/10.1063/1.4868256
View Table of Contents: http://scitation.aip.org/content/aip/journal/pof2/26/3?ver=pdfcov
Published by the AIP Publishing

PHYSICS OF FLUIDS **26**, 031702 (2014)

Axis-switching of a micro-jet

Juan Martin Cabaleiro[1,a)] and Jean-Luc Aider[2,b)]
[1]*Fluid dynamics Laboratory, Faculty of Engineering, University of Buenos Aires, Av. Paseo Colón 850, Buenos Aires, Argentina and Micro and Nanofluidics and Plasma Laboratory, Faculty of Engineering, Marina Mercante University, Av. Rivadavia 2258, Buenos Aires, Argentina*
[2]*Laboratoire de Physique et Mécanique des Milieux Hétérogènes (PMMH), UMR7636 CNRS, Université Pierre et Marie Curie (UPMC), Université Paris Diderot (UPD), École supérieure de physique et de chimie industrielles (ESPCI), de la Ville de Paris, 10 rue Vauquelin, 75231 Paris Cedex 05, France*

(Received 2 October 2013; accepted 20 February 2014; published online 11 March 2014)

In this study, it is shown that free microjets can undergo complex transitions similar to large-scale free jets despite relatively low Reynolds numbers. Using an original experimental method allowing for the 3D reconstruction of the instantaneous spatial organization of the microjet, the axis-switching of a micro-jet is observed for the first time. This is the first experimental evidence of such complex phenomena for free micro-jets. Combining these experimental results with Direct Numerical Simulations it is shown that the mechanism responsible for the axis-switching is the deformation of a micro-vortex ring due to induction by the corner vortices, as it occurs in large scale non-circular jets. © *2014 AIP Publishing LLC*. [http://dx.doi.org/10.1063/1.4868256]

Micro-jets are jets whose at least one dimension is lower than 1 mm. Their study and use have become more and more popular because of their great potential for flow control, especially control of separated flows. For instance, it was shown recently that using MEMS (Micro Electro Mechanical Systems) pulsed micro-jets to control the separated flow over the rear slant of a Ahmed body ensure a much better energy gain compared to macro-jets.[1] Unfortunately, pulsed micro-jets are both difficult to design and build using the MEMS technology. The expected pulsed jet frequencies and velocities for flow control application are very demanding for a MEMS. For aeronautics applications very high jet velocities (up to 300 m s^{-1}) and very high pulsed jet frequencies (up to 500 Hz or even 1 kHz) are needed. Apart from the technological difficulties, the physicists and experimentalists are also facing new challenges.

Because of the very small dimensions of the micro-nozzles, the investigation of the physical properties of micro-jets is very difficult. Using intrusive measurement devices like hot-wire anemometry is not satisfactory, especially close to the exit of the micro-nozzle. Seeding the fluid with oil micro-droplets is not possible because of the interaction with the walls and possible interactions with the micro-actuator. New or specific experimental techniques have to be considered to have access to the instantaneous and/or time averaged characteristics of the micro-jet.

For the same reason, very little is known about the micro-jets. Even if the dimensions of the micro-jet are small, the high jet velocities U_j ($U_j > 1$ m s^{-1}) often lead to relatively large Reynolds numbers, or at least unusually large Reynolds numbers $Re_j = U_j d/\nu$ (d being the micro-jet diameter, ν the kinematic viscosity of the fluid) for micro-flows: $Re_j = 3500$ for $U_j = 100$ m s^{-1} and $d = 4 \times 10^{-4}$ m. In this range of Reynolds numbers, instabilities and transitions are expected, which is very unfamiliar in the world of micro-flows. It is also very difficult to measure large velocities at the sub-millimeter scale. For these reasons, the dynamics and transition of micro-jets is a new and interesting research field which is related to the more general problem of gas flows at the micro-scale and in MEMS (cf. the GasMEMS network supported by the FP7 of the European Commission).

a)jmcabaleiro@fi.uba.ar
b)aider@pmmh.espci.fr

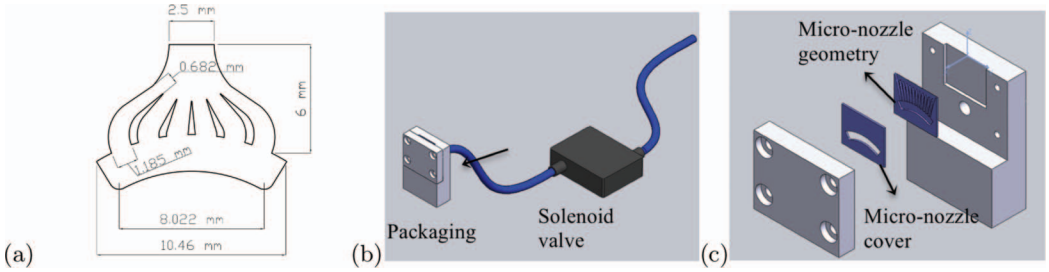

FIG. 1. (a) Main planar dimensions of the MEMS micro-nozzle which is 380 μm thick. (b) The incoming flow is pulsed using a solenoid valve. (c) The packaging has been designed to make as simple as possible the modification of the micro-jet geometry. (b) and (c) Reprinted with permission from Cabaleiro *et al.*, J. Visualization **16**, 263–274 (2013). Copyright 2013 Springer Science and Business Media.

At large scales, it is well-known that free-jets can exhibit very complex features, depending on the jet velocity U_j. The shear layers growing around the jet play a significant role in the transition process through the creation of strong Kelvin-Helmholtz vortices. The structures created in the shear layers surrounding the jet usually develop as vortex rings.[2] Whatever the shape of the outlet section of the nozzle, vortex rings are created and advected along the jet axis. Their interaction and destabilization lead to the final transition to turbulence of the jet. The transitions of the macro-jets being intrinsically associated with vortex generation, one can wonder about their existence when considering small scales, lower Reynolds number micro-jets. Gau *et al.*[3] proposed one the first experimental study of continuous micro-jets and showed that no vortex structures could be observed in their velocity range ($0.5 < U_j < 50$ m s^{-1}).

Among the peculiar phenomena observed in a free-jet, axis switching is one of the most spectacular: for rectangular or elliptic jet sections, one can observe a 90° shift in the jet's principal axis of symmetry. It was observed experimentally by Hussain and Hussain[4] and Hertzberg and Ho[5] then numerically by Grinstein.[6] Theoretical and stability analysis has been used (e.g., by Abramovich[7] and by Koshigoe *et al.*[8]) to explain axis switching in terms of the jet shear layer having different growth rates in the characteristic directions. Hussain and Hussain[4] have shown experimentally that azimuthal vorticity plays a critical role in axis switching. Later, Grinstein[6] confirmed numerically that axis-switching could be explained by self-induction of the vortex rings created around the jet. The role of azimuthal vortical structures in axis switching was emphasized experimentally by Zaman.[9] He also showed that axis switching could be strongly perturbed when using tab vortex generators. Recently, a 3D reconstruction of an axis switching jet was performed in the context of phonation-related studies, for the 3D velocity field of a high aspect ratio jet.[10] The rates of growth of the jet in the two symmetry planes of the nozzle were shown to obey self-similarity principles, which make them inter-dependent.[11] All these experimental and numerical studies agree on one point: if there are no vortex structures, then axis switching should not be possible. Following the recent observation of Gau *et al.*[3] who found no vortical structures in their experimental study, then one can wonder whether axis switching is possible for micro-jets.

The objective of the present study is to show that axis-switching can occur in micro-jet flows. In this purpose, we studied the 3D structure and dynamics of a pulsed micro-jet generated by a MEMS actuator which was used in flow control experiments.[1] For the present study, a hybrid configuration was used. The jet micro-nozzle is strictly the same as the MEMS actuator. It is made using a SOI (Silicon On Insulator) wafer and MEMS fabrication processes to ensure the same dimensions for the micro-nozzle. The geometry and the principal planar dimensions of the convergent micro-nozzle are presented in Fig. 1(a), where the rest of the dimensions are in scale. The micro-jet cross-section is rectangular. The micro-nozzle thickness l_j is 380 μm thick (x axis). The length L_j of the outlet section is 2.5 mm long (y axis). The aspect ratio $AR = \frac{L_j}{l_j}$ is then 6.5. The jet grows along the z axis and it is pulsed using a fast solenoid valve (Matrix^{TM}) just upstream the micro-jet nozzle (Fig. 1(b)). The pulsation frequencies F_j can range between 1 and 500 Hz.

As mentioned in the Introduction, characterization of high-speed micro-jets is challenging because of the very small scales and high velocities of the flow. To visualize the instantaneous 3D

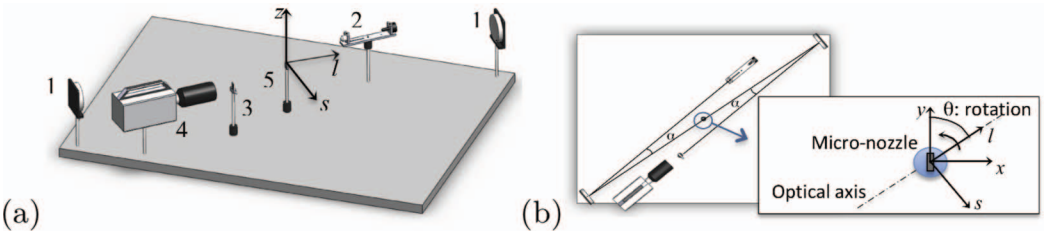

FIG. 2. (a) Sketch of the optical setup used for the Schlieren visualization. (b) The rotation of the jet around its axis and phase averaging of multiple planar visualization allows for the 3D reconstruction of the pulsed micro-jet. Reprinted with permission from Cabaleiro *et al.*, J. Visualization **16**, 263–274 (2013). Copyright 2013 Springer Science and Business Media.

structure of the micro-jet, a dedicated experimental setup and methodology has been developed by Cabaleiro *et al.*[12] To avoid seeding the flow (Particle Image Velocimetry) and to avoid intrusive devices (hot wire velocimetry), a Schlieren setup was used (Fig. 2(a)). The working fluid is helium to ensure a good refractive index difference with surrounding air. The flow is visualized using a high sensitivity high-speed camera (Photron SA4) with an acquisition frequency F_{ac} up to 20 kHz, depending on the size of the recorded image. In this work, the acquisition frequency was $F_{ac} = 8$ kHz. The spatial resolution was 0.1 mm/px, and the image size was of 320 × 464 pixels.

The Schlieren setup shown in Fig. 2(a) gives access to instantaneous 2D visualizations of the micro-jet with a high spatial and temporal resolution. To have access to the instantaneous 3D structure of the jet, the jet is rotated around its axis and flow visualization is made every $\theta = 5^{\circ}$ (Fig. 2(b)). 3D reconstruction is then obtained using a Filtered Back Projection algorithm. Phase averaging is used to ensure a better image quality at each time step. The methodology is fully detailed and validated in Cabaleiro *et al.*[12]

The 3D structure of the flow generated by the convergent micro-nozzle is investigated for a given pulsation frequency $F_j = 20$ Hz (T = 0.05 s) with a duty cycle $dc = 0.5$ and for a given pressure of 30 mbar. The corresponding maximum jet velocity is $U_j = 10.4$ m s^{-1} leading to $\mathrm{Re}_j = 263.5$, based on the nozzle thickness and on helium's viscosity at ambient temperature.

The evolution of 3D iso-surfaces during the part of the cycle when the jet is open is shown in Fig. 3. One can clearly see the front of the starting jet rising from the jet nozzle at the beginning of the cycle. The jet velocity has been estimated by tracking this front during the first time steps. The iso-surface grows along the jet axis. For this aspect ratio, the structure of the micro-jet looses its rectangular shape and a clear deformation appears along the direction perpendicular to the long axis of the rectangular nozzle almost immediately after the cycle starts. This deformation is visible for the rest of the open half cycle. Four horizontal cross-sections of the iso-surface obtained at time 10 ms (Fig. 3(d)) are shown in Fig. 4 for increasing positions along the jet axis. The beginning of

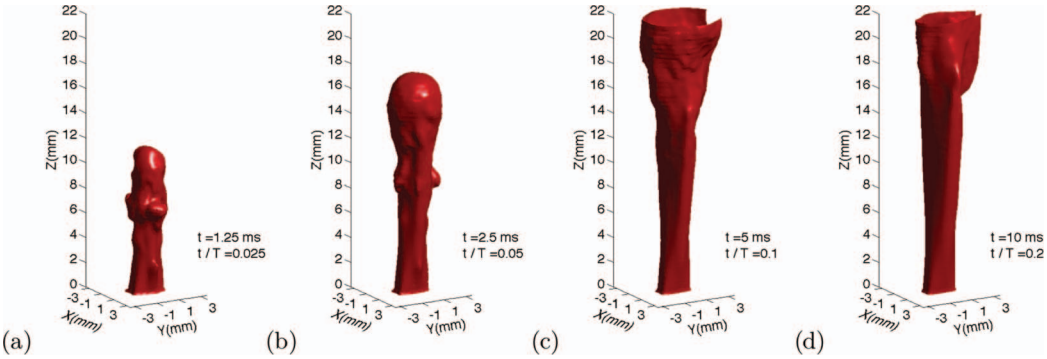

FIG. 3. Time evolution of the pulsed micro-jet 3D structure over one pulsation cycle for $F_j = 20$ Hz and $U_j = 10.4$ m s^{-1} ($\mathrm{Re}_j = 263.5$) (Multimedia view). [URL: http://dx.doi.org/10.1063/1.4868256.1]

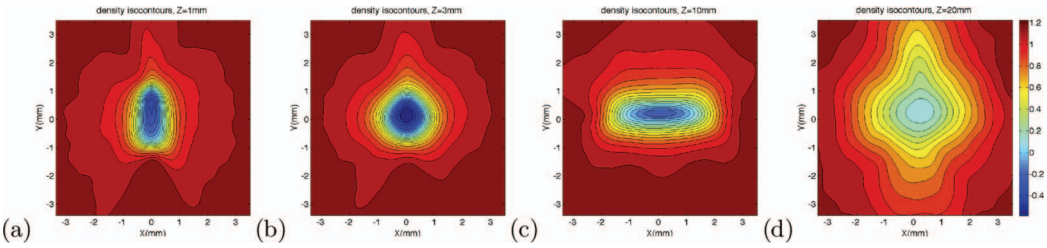

FIG. 4. Spatial evolution of the density contours in different cross-sections along the jet axis at time 10 ms. $F_j = 20$ Hz and $U_j = 10.4$ m s^{-1} (Re$_j = 263.5$).

axis switching is well-defined. In Fig. 4(b), a diamond shape appears in the iso-density contours. It corresponds to the beginning of the switching which occurs around $z = z_{switch} \approx 3$ mm.

It is possible to define more precisely z_{switch}, the position along the jet axis where the axis switching occurs. Using the 3D reconstruction, the frontier defining the jet along the x and y axes can be followed along the jet axis (z). The result is shown in Fig. 5(a) where the jet width along the x (Δx) and y (Δy) axes are plotted as a function of z ($t = 10$ ms). At $z = 0$, the dimensions of the convergent nozzle are recovered ($\Delta x = 0.38$ mm and $\Delta y = 2.5$ mm). The axis switching can be defined as the position along the z axis where Δx and Δy crosses, i.e., $z_{switch} = 3$ mm in Fig. 5(a). A second switch is also found further downstream at $z = z_{switch2} = 17.4$ mm. In this case, the jet breakdown takes place much further from the axis switching, out of the observed region.

It is also interesting to plot the positions of the axis switchings as a function of time to analyze whether it is the switching of a transient structure, or if the switching remains after the initial transient. In the case of this convergent micro-nozzle, it can be seen both in the iso-surface evolution presented in Figs. 3 and 5(b) that the first switching position (closest to the nozzle exit) evolves only during the first 5 ms, and then remains fixed until the end of the cycle. This is a first indication that at least the part of the jet closer to the nozzle has reached steady state after 5 ms. This is not the case for the position of the second switch which moves further away from the nozzle exit with time. The same analysis has been carried out for a lower Reynolds number (Re$_j = 137$). The evolution of the first axis switching was similar to the one described for the Re$_j = 263.5$ case, but the second switch could not be observed anymore.

Our experimental observations are clear: axis switching of jets occurs even at the micro-scale. The question is then: how can it be explained if the flow is indeed vortex-free as suggested by Gau, Shen, and Wang[3] ? Our experimental setup is well-adapted for a qualitative analysis of the 3D structure of the jet, but it does not give access to the vorticity field. This is the reason why a

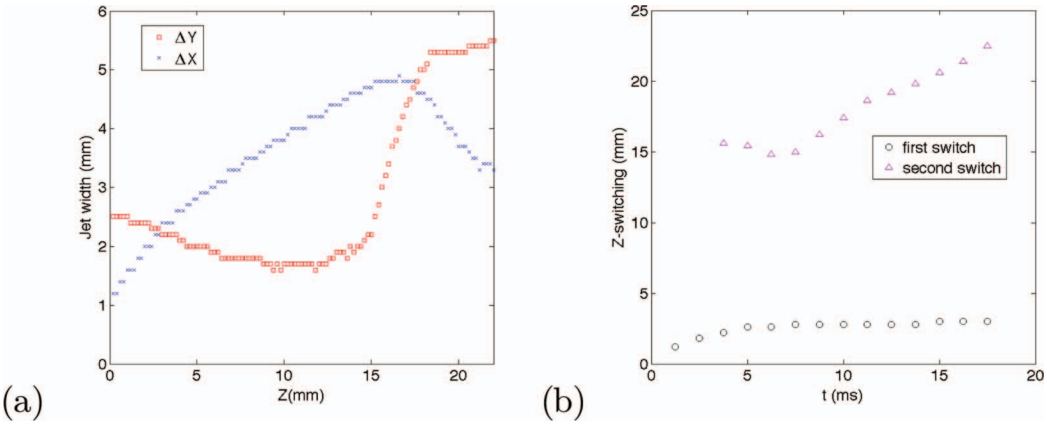

FIG. 5. (a) Evolution of the length and width of the micro-jet generated by a convergent micro-nozzle at $t = 10$ ms. The location of axis switching $z_{switch} = 3$ mm is very well defined. (b) Evolution of the first and second axis switching positions of the micro-jet for $U_j = 10.4$ m s^{-1} (Re$_j = 263.5$).

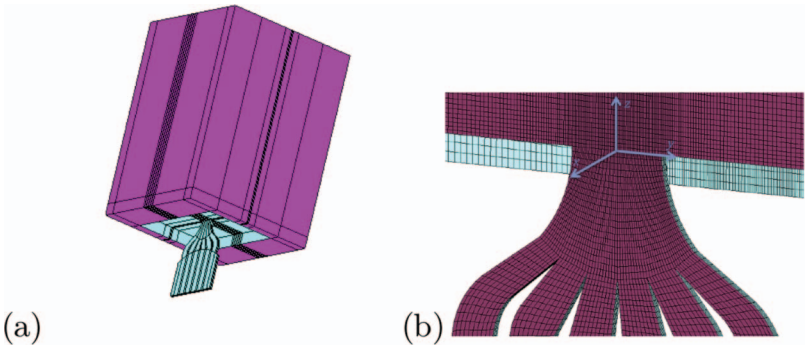

FIG. 6. (a) CAD view of the 3D computational domain used for the DNS. (b) Zoom in view of the structured mesh near the nozzle exit.

Direct Numerical Simulation (DNS) of the micro-jet flow has been carried out. A finite volumes code developed by Electricité de France (EDF), called Code Saturne,[13] was used to run a 3D time-dependent simulation for the same Reynolds number ($Re_j = 263.5$). Fig. 6(a) shows the 3D geometry and computational domain used for the simulation. To make the comparison more meaningful, the flow into the micro-nozzle is also computed to ensure that the velocity profiles are fully developed at the exit of the jet nozzle. The inflow condition at the inlet of the micro-nozzle is a constant velocity profile corresponding to the first half of the pulsation where the jet is fed at constant pressure and then is strictly similar to a continuous jet. The micro-jet can grow freely into a large volume whose boundaries are defined as free outlet conditions. The large computational domain is 3 cm long (axial direction), 2.2 cm thick, and 2.2 cm wide. We used a 4×10^6 volumes structured mesh which is refined in the shear layers regions. The size of the smallest grid cell is 38 μm, corresponding to 10 cells along the thickness of the jet nozzle. A detailed view of the structured mesh is presented in Fig. 6(b).

Fig. 7(a) shows the axial velocity profiles along $x = 0$ and $y = 0$ axes at the exit of the micro-nozzle ($z = 0$) at t = 10 ms. One can see that a Poiseuille type velocity profile is indeed recovered at the exit of the micro-nozzle. The time evolution of the exit axial velocity profiles along the y direction at $x = 0$ mm and $z = 0$ mm ($V_z(0, y, 0, t)$) is presented in Fig. 7(b). The modulations along the y direction are due to the presence of the guiding vanes in the micronozzle (Fig. 1(a)). A temporal evolution of the axial velocity at different axial positions z_i along the jet's axis ($V_z(0, 0, z_i, t)$) is shown in Fig. 7(c). Finally, the axial velocity along the jet's axis ($V_z(0, 0, z, t_i)$) is presented in Fig. 7(d) at several times t_i. From these velocity profiles one can see that the microjet has reached steady state in most of the domain at $t = 10$ ms, which is one fifth of the period (T = 50 ms).

Because our experimental visualizations are based on density isocontours, the transport of a passive scalar was also computed to visualize the flow in the simulation. The evolution of the jet is shown in Fig. 8 through four snapshots of iso-surfaces of the passive scalar. The scales shown in these figures are nondimensional based on the nozzle thickness l_j ($X^* = x/l_j$, $Y^* = y/l_j$, $Z^* = z/l_j$). The flow structure obtained at the four time steps is very similar to the ones found in the experiment. The most important result is that the numerical simulation also exhibits a clear axis-switching of the micro-jet. Moreover, the deformation of the front is well recovered. It allows us to analyze the velocity field to find out whether vortical structures exist or not.

The vortical structures found in the instantaneous 3D velocity fields are visualized by using the λ_2 criterion as defined in Jeong and Hussain.[14] The result is shown in Fig. 9. It can be observed that there are indeed ring vortices created at the very first stage of the jet ejection. They are very similar to the ones found by Grinstein[2]. One can witness clearly the switching of a ring vortex whose diameter is smaller than 1 mm. It demonstrates that the axis switching can be explained by the mechanism of induction created by the corner vortices even for low Reynolds number micro-jets.

In the present study, a dedicated experimental setup has been used to investigate the instantaneous 3D structures of pulsed micro-jets. Schlieren visualizations together with a Filtered Back Projection algorithm allow for precise 3D reconstruction of the 3D structures of the micro-jet at high frame

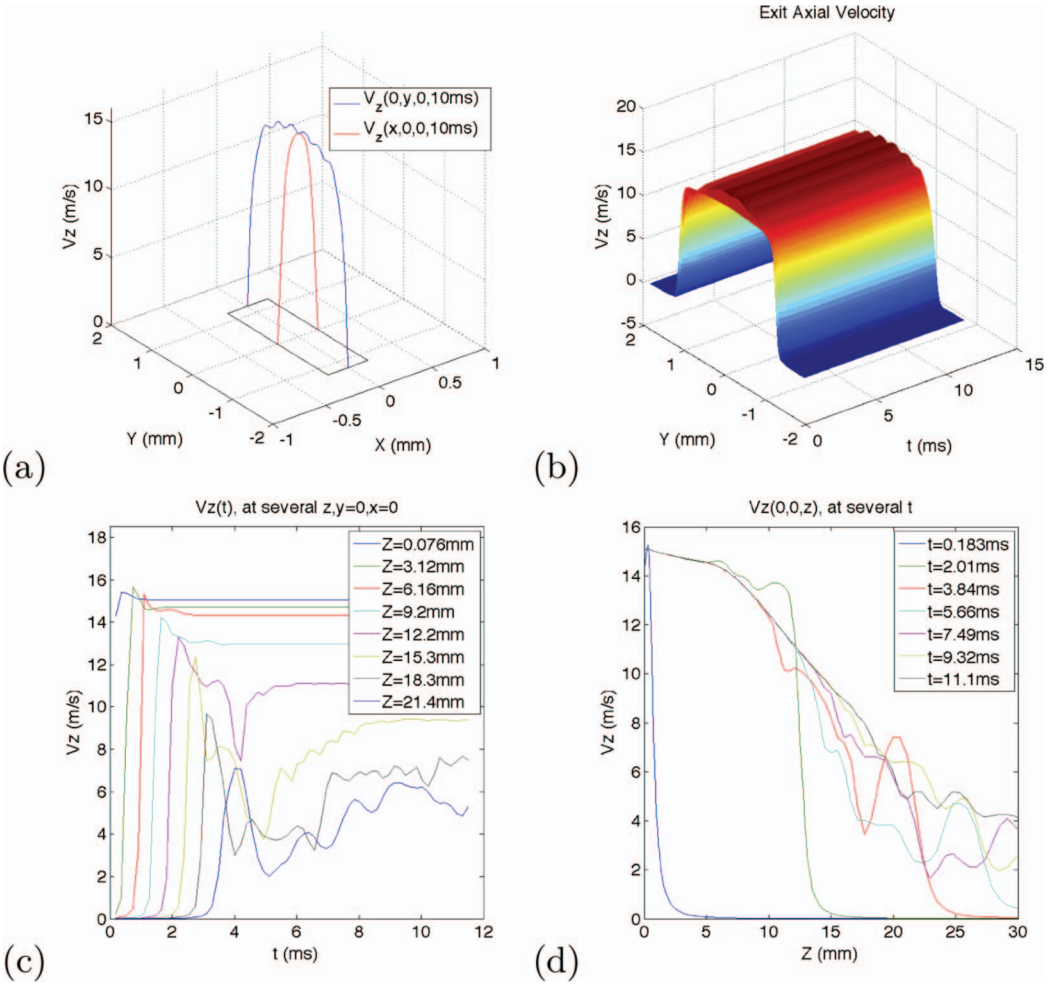

FIG. 7. (a) Axial velocity profiles along $x = 0$ and $y = 0$ axes at the exit of the micro-nozzle ($z = 0$) at t = 10 ms. A Poiseuille profile is recovered along the x direction. (b) Temporal evolution of the axial velocity at the nozzle exit. (c) Temporal evolution of the axial velocity at the several points along the jet's axis. (d) Axial velocity profiles along the jet's axis for seven time steps.

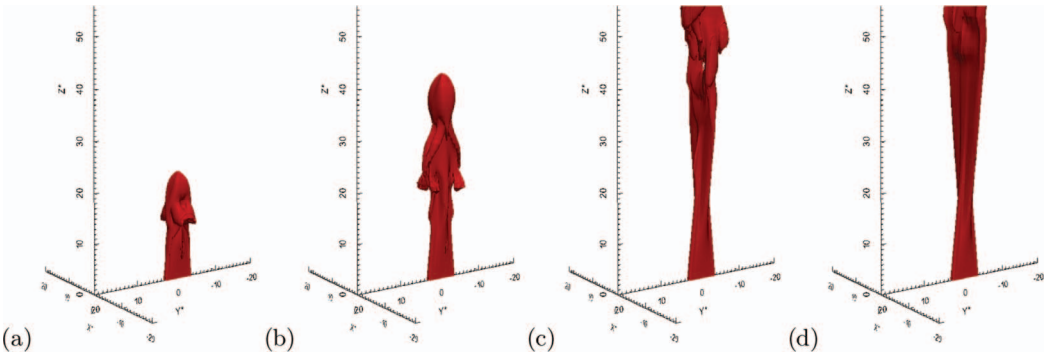

FIG. 8. Numerical simulation of the pulsed micro-jet. A passive scalar is used to visualize the micro-jet and follow its time evolution. These frames correspond to the same times presented in Fig. 3. $Re_j = 263.5$.

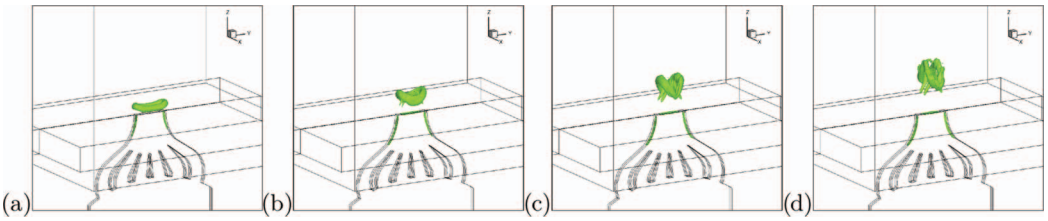

FIG. 9. Numerical simulation of the pulsed micro-jet. Visualization of a micro-vortex ring using λ_2 isocontours for $Re_j = 263.5$. Its time evolution shows its creation, deformation, and switching. (a) t = 0.18 ms (t/T = 0.0036). (b) t = 0.36 ms (t/T = 0.0072). (c) t = 0.54 ms (t/T = 0.0108). (d) t = 0.72 ms (t/T = 0.0144).

rates (up to 8 kHz in the present experiments). The convergent geometry of the micro-nozzle is most favorable to axis-switching. In this case, axis switching takes place very close to jet exit. For $Re_j = 263.5$, a second switching has been observed. This is the first experimental evidence of the existence of axis switching of micro-jets. In order to find an explanation to this experimental result, a DNS has been performed. The axis switching was also observed in the numerical simulation. A micro-vortex ring could then be visualized in the early stage of the starting jet. The deformation of the micro-vortex clearly demonstrates that the mechanism responsible for the axis switching is that of induction by the corner vortices, even for these low Reynolds numbers and small scales configurations. The axis switching of micro-jets has been clearly demonstrated both experimentally and numerically. The numerical simulation allows for a better understanding of the phenomena through the visualisation of vortex rings which are impossible to measure because of the small scales and large velocities of the micro-jet. Finally, from the flow control point of view, it confirms the difficulty in evaluating the performances of MEMS micro-jets. Indeed, the present results show that conventional velocimetry techniques can be highly misleading. If axis switching occurs, local or 2D measurements may lead to a strong underestimation of the micro-jet velocity.

ADEME is gratefully acknowledged for its financial support (CARAVAJE project). This work has also been supported in part by the Argentinian ANPCyT through the project PRH-PICT 2008-250 and by the LIA PMF-FMF (French-Argentinian International Associated Laboratory in Physics and Fluid Mechanics).

[1] P. Joseph, X. Amandolese, C. Edouard, and J.-L. Aider, "Flow control using MEMS pulsed micro-jets on the Ahmed body," Exp. Fluids **54**, 1442 (2013).
[2] F. F. Grinstein, "Vortex dynamics and entrainment in rectangular free jets," J. Fluid Mech. **437**, 69–101 (2001).
[3] C. Gau, C. H. Shen, and Z. B. Wang, "Peculiar phenomenon of micro-free-jet flow," Phys. Fluids **21**, 092001 (2009).
[4] F. Hussain and H. S. Husain, "Elliptic jets. Part 1. Characteristics of unexcited and excited jets," J. Fluid Mech. **208**, 257–320 (1989).
[5] J. R. Hertzberg and C. M. Ho, "Three-dimensional vortex dynamics in a rectangular sudden expansion," J. Fluid Mech. **289**, 1–27 (1995).
[6] F. F. Grinstein, "Self-induced vortex ring dynamics in subsonic rectangular jets," Phys. Fluids **7**, 2519 (1995).
[7] G. Abramovich, "Deformation of the transverse section of a rectangular turbulent jet," Fluid Dyn. **18**, 40–48 (1983).
[8] S. Koshigoe, E. Gutmark, K. C. Schadow, and A. Tubis, "Initial development of noncircular jets leading to axis switching," AIAA J. **27**, 411–419 (1989).
[9] K. B. M. Q. Zaman, "Axis switching and spreading of an asymmetric jet: The role of coherent structure dynamics," J. Fluid Mech. **316**, 1–27 (1996).
[10] F. Krebs, F. Silva, D. Sciamarella, and G. Artana, "A three-dimensional study of the glottal jet," Exp. Fluids **52**, 1133–1147 (2012).
[11] D. Sciamarella, F. Silva, and G. Artana, "Similarity analysis of a glottal-like jet," Exp. Fluids **53**, 765–776 (2012).
[12] J. Cabaleiro, J. Aider, G. Artana, and J. Wesfreid, "Single camera time-resolved 3d tomographic reconstruction of a pulsed gas jet," J. Visualization **16**, 263–274 (2013).
[13] F. Archambeau, N. Méchitoua, and M. Sakiz, "Code saturne: A finite volume code for the computation of turbulent incompressible flows," Int. J. Finite **1** (2004).
[14] J. Jeong and F. Hussain, "On the identification of a vortex," J. Fluid Mech. **285**, 69–94 (1995).